EFFECTS OF FIBRE SIZING ON DAMAGE DEVELOPMENT IN UNIDIRECTIONAL GLASS/EPOXY COMPOSITES

M. Kharrat [1,3], T. Monlèon [1,2], L. Carpentier [3], A. Chateauminois [1] and M.L. Maspoch[2]

[1] *Laboratoire d'Ingéniérie et Fonctionnalisation des Surfaces*
Ecole Centrale de Lyon, BP 163, 69131 Ecully Cedex, France
[2] *Departament de Ciència dels Materials i Enginyera Metal-lurgica*
Universitat Politècnica de Catalunya, 647 Avda Diagonal, 08028 Barcelona, Spain
[3] *Laboratoire de Tribologie et Dynamique des Systèmes*
Ecole Centrale de Lyon, BP 163, 69131 Ecully Cedex, France

SUMMARY:. The micro and macro mechanical behaviour of unidirectional glass/epoxy composites differing by their fibre sizing has been investigated. Three different model sizing have been considered: A1100 only, A1100 with an epoxy prepolymer (DGEBA) and A1100 with a linear polyurethane (PU). The composite based on the A1100/PU sizing was characterised by a much greater sensitivity to damage development under impact and fatigue loading in flexural mode. This difference was related to a low shear strength, which induced an enhanced delamination under mechanical loading. On the other hand, micro-indentation tests were unable to reveal any difference in the fibre/matrix interfacial shear strength. The low macro-mechanical properties of the A1100/PU composite were interpreted by considering the highly heterogeneous fibre distribution which resulted from the low wettability of the sizing by the epoxy matrix. The main effect of the sizing was thus to affect the impregnation process during manufacturing, rather than modifying the intrinsic mechanical properties of the interface.

KEYWORDS: Fibre sizing; interface; fatigue; strength; micro-indentation; micro/macro mechanical properties; Glass/epoxy

INTRODUCTION

The major contribution of the interface between fibres and polymers – or the so-called interphase – has been widely recognised since the early days of synthetic fibre composites. It has especially been demonstrated that damage development in composite subjected to mechanical loading is strongly dependent upon the strength of the interface (see [**1**] for example). The prediction of composite durability thus rely largely on the assessment of the mechanical properties of the interface in relation to fibre treatments and processing conditions.

Two major routes can be used to investigate interfacial properties. The first one relies on macro-mechanical tests carried out under loading conditions where the interface shear

response is enhanced (off-axis tensile tests, short beam bending tests…). The resulting mechanical behaviour, is, however, dependent upon many extraneous factors such as fibre misalignments, void content…As a result, several doubts surround the extraction of intrinsic interface properties from such macro-mechanical tests [**2**].
Direct investigations of the interfacial behaviour at the micro-mechanical level have thus received a growing interest over the past years. Except for the micro-indentation technique, most of the existing tests (fragmentation, pull-out, droplet micro-tension) involves model systems based on a single filament embedded into a polymer matrix. In such systems, the description of the real physico-chemical state of the interface in a composite remains questionable. Moreover, some controversial has recently emerged regarding the failure mode of the interface. Although great progress has been made with fracture analysis of interface failure, it has been pointed out that the centro-symmetry of single filament micro-mechanical tests is unable to reproduce the interface failure modes really encountered in composites [**3**].
The purpose of this study was thus to investigate some of the aspects of the correlation between macro and micro-mechanical behaviour in the case of glass/epoxy composites. The emphasis was put on the potential of a combination of micro and macro-mechanical testing to assess the effects of fibre sizing on the damage resistance of unidirectional composites. The study of the macro-mechanical behaviour was focused on damage development under dynamic loads (fatigue, impact) which are known to be very sensitive to the interface strength. Micro-mechanical tests were carried using a micro-indentation test which presents the advantage of using real composites. Composites with different model sizing have been elaborated and the correlation between microscopic and macroscopic behaviour was analysed in the light of the materials microstructure.

RESULTS AND DISCUSSION

Materials and experimental details

Materials

Unidirectional glass/epoxy composites were used for this study. The matrix was obtained from a diglycidil ether of bisphenol-A (DGEBA) resin (CIBA LY556), which was cured using a stoichiometric amount of isophorone diamine hardner (IPD, Hüls).The reinforcement was an E-glass roving (800 tex) supplied by Vetrotex International. Prior to impregnation, the fibres were coated with γ-aminopropyl triethoxysilane (A1100) based sizing. Three different model sizing have been selected:

i) a sizing containing A1100 only (denoted as S1),
ii) a sizing including an epoxy prepolymer (DGEBA) in addition to A1100 (denoted as S2),
iii) a sizing containing A1100 and a linear polyurethan (denoted as S3).

The weight fractions of the sizing layer on the fibres were respectively 0.03%, 1.1% and 0.46% for S1, S2 and S3. From a previous physico-chemical investigation by Lacrampe[**4**], S1 and S2 were expected to give a glassy interface of limited thickness. On the other hand, the S3 sizing was only poorly miscible within the epoxy matrix and it was therefore supposed to give a thicker interphase, with a lower crosslinking density and glass transition temperature.
Unidirectional plates 3 mm thick have been elaborated by filament winding. The cure cycle was 2.5 h at 140 °C followed by 15 mn at 165 °C. Fibre volume fractions, void fractions and glass transition temperatures (T_α, measured at 1 Hz by D.M.T.A.) are reported in Table 1. Depending on the sizing composition, the glass fibres did not exhibit the same wettability by

the epoxy resin during the impregnation step. As a result, it was not possible to achieve exactly the same fibre fraction and void content for the three different composites. Specimens 100 x 10 mm^2 were cut out from the plates for all the mechanical tests.

Table1: *Fibre fractions, voids content and temperatures of the α thermo-mechanical transition of the composites (1 Hz, 1°/min).*

Sizing	Fibre volume fraction (%)	Void fraction (%)	T_α (°C)
A1100 only	41	3.3	165.7
A1100 + DGEBA	37	4.8	167
A1100 + PU	49	7.3	161.3

Fatigue tests

Dynamic fatigue tests were performed under three-point-bending conditions at imposed sinusoidal displacement. The test frequency was set to 25 Hz with a strain ratio $R = \varepsilon_{min}/\varepsilon_{max}$ equal to 0.1 (ε_{min} and ε_{max} are respectively the minimum and the maximum strain during the fatigue cycle). A span-to-depth ratio equal to 20 was selected in order to minimise shear stresses. The stiffness-loss curves were continuously recorded as a function of the number of cycles using a load cell located below the loading nose. A 10% decrease in the relative stiffness was chosen as a conventional lifetime criterion. Using this criterion, it was still possible, at the end of the test, to identify the original damage mechanisms that led to sample failure.
In addition to fatigue testing, quasi-static flexural properties have been measured using the same span-to-depth ratio and a cross-head speed of *ca.* 2 $mm.mn^{-1}$. The Inter-Laminar Shear Strength (ILSS) was also measured at the same loading rate using a span-to-depth ratio equal to 5.

Impact tests

Impact tests have been performed using a conventional 'Charpy' impact testing machine. Specimens were tested under a three point bending configuration with a 50 mm span. The impact energy was set to 50 J.

Micro-indentation testing

Micro-indentation has been carried out using a specific device described elsewhere [**5**]. Tests were performed using thick (10mm) polished cross-sections of the composite plates. The loading was carried out at imposed displacement rate (0.2 $\mu m.s^{-1}$) using a Vickers diamond indenter. The normal load and the indenter displacement were continuously monitored during loading and unloading. The maximal load was set to a value of *ca.* 0.5 N, which was found to be sufficient to induce a systematic fibre debonding. The latter was checked after each test by means of optical microscope observations of the indented fibre. The occurrence of debonding was indicated by a black circle surrounding the edge of the fibre. Tests with fractured fibres were systematically discarded from data analysis.

Strength properties

The strength properties of the composites have been tested under quasi-static flexural conditions (Table 1). A slightly higher strain to failure was achieved with the DGEBA/A1100 (S2) sizing. If stresses to failure are considered, most of the observed differences can be attributed to the changes in the fibre content as the sizing was modified.
The most significant difference was related to the failure mode of composite S2. Whereas S1 and S3 specimens exhibited a progressive failure by fibre breakage and delamination from the tensile side, composite S3 failure was associated with a localised micro-buckling of the fibres beneath the loading nose. Such a mechanism is known to be due to an indentation effect of the loading nose, which induces locally high compressive and shear stresses on the compressive side of the specimen [**6**]. This kind of failure can therefore not be considered as truly representative of the intrinsic bending behaviour of the composite and it only provides an underestimated value of the flexural strength. These compressive mode failures have been found to be especially enhanced in the case of creep sensitive matrix, such as water plasticised epoxy [**7**]. In the present case, it can be noted that the composite S3 exhibited a lower α thermo-mechanical transition temperature than composites S1 and S2 (Table 1). This indicates a lower cross-link density of the epoxy matrix when a PU polymer was used in the sizing formulation. These lower thermo-mechanical properties could account for an higher sensitivity to creep and fibre micro-buckling beneath the loading nose during flexural loading.

Table 2: *Flexural strength and inter-laminar shear strength (ILLSS) properties of the composites. (standard deviations within brackets).*

Sizing	Stress to failure: σ_r (MPa)	Strain to failure: ε_r (%)	ILSS (MPa)
S1	920 (25)	3.05 (0.07)	72 (0.8)
S2	880 (50)	3.41 (0.15)	69 (4)
S3	1060 (40)	3.06 (0.17)	41 (0.7)

A strong difference was also noted between the ILSS properties of the composite S1 and S2 and those of the composite S3, which exhibited an anomalous low shear strength. This low shear strength of material S3 can be attributed to either a poor fibre/matrix adhesion or to macroscopic defects such as voids, which can act as stress concentrators. The possible contribution of voids to the observed premature shear failure is further supported by the high void content of composite S3 (Table1). At this stage, it is, however, not possible to differentiate between the respective contributions of the interface strength and the macroscopic defects to the macro-mechanical shear properties.

Impact behaviour

Under impact testing, a strong difference in the failure mechanisms was also observed between composite S1 and S3 (No tests were carried out with material S2). Composite S1 exhibited a localised failure close to the impacter, which involved mostly fibre breakage from the tensile side of the specimens. On the other hand, S3 failed in a shear mode along the mid-plane of the samples, with a only limited damage on the tensile side of the specimens. This difference in failure modes resulted in very different impact resistance (182 kJ/m^2 for composite S1 and 331 kJ/m^2 for composite S3). The highly dissipative shear failure of composite S3 can be related to its low ILSS.

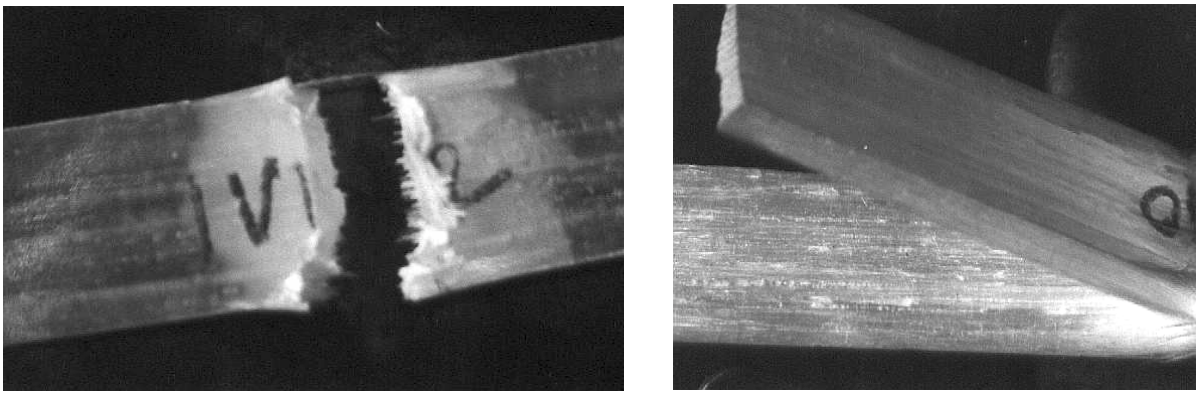

(a) (b)

Fig. 1: *Failure modes of composites S1 (a) and S3 (b) under impact testing.*

Fatigue behaviour

Three point bending tests have been carried out using composites S1 and S3. fatigue data have been reported in conventional S-N diagrams giving the maximum applied strain ε_{max} as a function of the lifetime criterion N_{10}.(Fig. 2 and 3).
In the investigated strain range, the fatigue behaviour of the material S1 can be described using a Wöhler's relationship:

$$\varepsilon_{max} = A - B \log N_{10} \quad (1)$$

with A and B are constants equal to 5.2% and 0.5%/decade respectively.

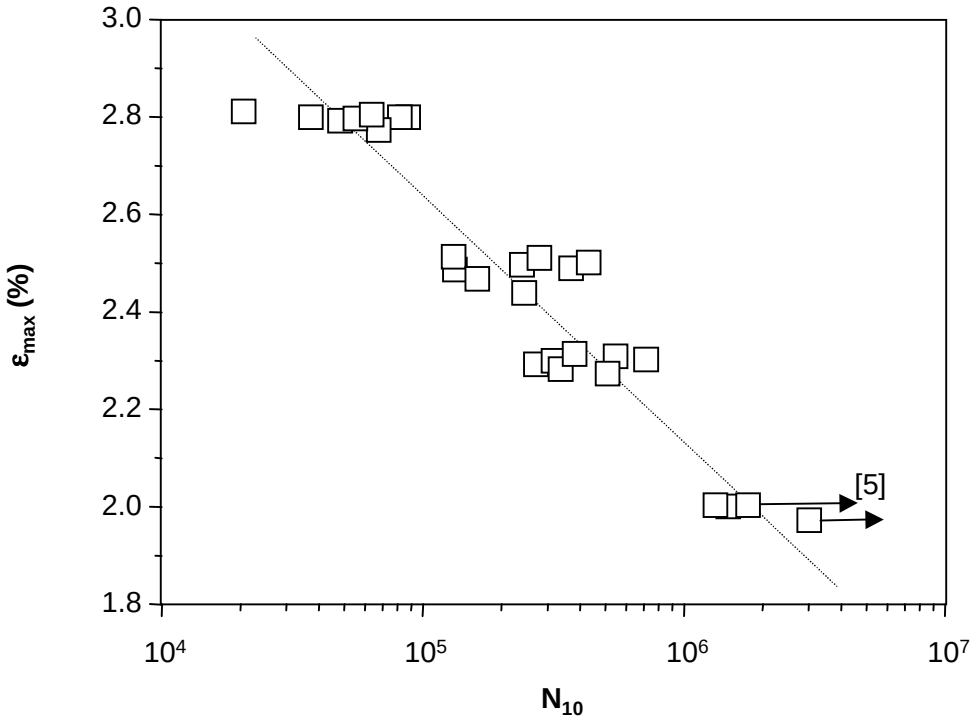

Fig. 2 : *S-N fatigue curve of composite S1.*
(Arrows correspond to run-outs).

Fatigue damage was associated with progressive fibre failure and bundle delamination from the tensile side of the specimens.
For composite S3, this tensile failure mode was obtained only at the lowest strain levels (ε_{max}<2.0 %). At higher strain values, a very unusual shear failure was observed along the specimen mid-plane, despite the fact that a large span-to-depth ratio was selected in order to minimise shear stresses. This delamination occurred well below the strain corresponding to the compressive (micro-buckling) mode failure under quasi-static loading (cf. Table 2). This tends to demonstrate that flexural fatigue behaviour was especially sensitive to the poor shear resistance of the material S3.
The comparison between the Wöhler's curves of composites S1 and S3 was restricted to the specimens which exhibited the same failure mode, i.e. tensile breakage. For composite S3, A and B values were found equal to 3.2% and 0.3%/decade respectively. The low A value indicated that even the tensile fatigue failure was enhanced by the S3 sizing.

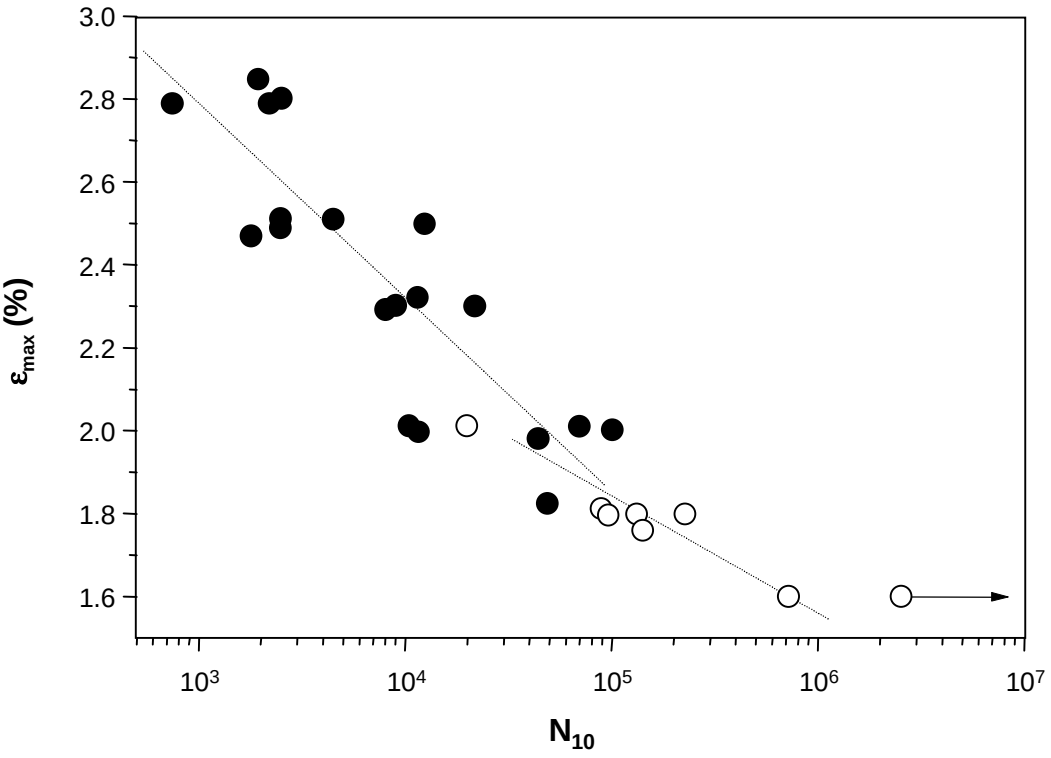

Fig. 3 : *S-N fatigue curve of composite S3.*
(①):delamination; (⑨) tensile failure.
(Arrows correspond to run-outs).

Micro-indentation testing

Micro-indentation tests have been performed using the three different materials. As previously reported [**5,8**], the indentation curves giving the normal load as a function of the applied indenter displacement do not show any sharp discontinuity associated to fibre debonding. A specific procedure was therefore used to assess the interfacial shear strength. It involved two steps:

(i) the subtraction from the overall measured displacement of the displacement component due to the elasto-plastic indentation of the fibre surface by the Vickers indenter. The latter was assessed from indentation tests carried out using bulk E-glass. This treatment of the raw data

resulted in 'reduced' indentation curves giving the elastic displacement u_o of the fibre surface as a function of the applied load P. The reduced indentation curves systematically exhibited a non linear behaviour (Fig. 4) which was associated with the progressive debonding of the fibre.

(ii) a shear-lag model taking into account the occurrence of debonding was used to assess the interfacial shear strength τ_i from the reduced indentation curves. The following two expressions have been derived for the loading step :

$$F<F_d \qquad u_o = \frac{\sigma_o}{nE} \tag{2}$$

Where F_d is the debonding load, σ_0 is the nominal applied stress ($P/\pi a^2$), E is the fibre Young's modulus and a is the fibre diameter. n is given by :

$$n = \sqrt{\frac{2k}{aE}} \tag{3}$$

where k is a global stiffness constant including the elastic properties of the matrix as well as the environment of the fibre.

$$F>F_d \qquad u_o = \frac{1}{2nE}\left(\frac{\sigma_o^2}{\sigma_d} + \sigma_d\right) \tag{4}$$

Where σ_d is the debonding stress. Full details regarding the extraction of reduced indentation curves and the derivation of the shear lag model can be found in refs [**5**] and [**9**].

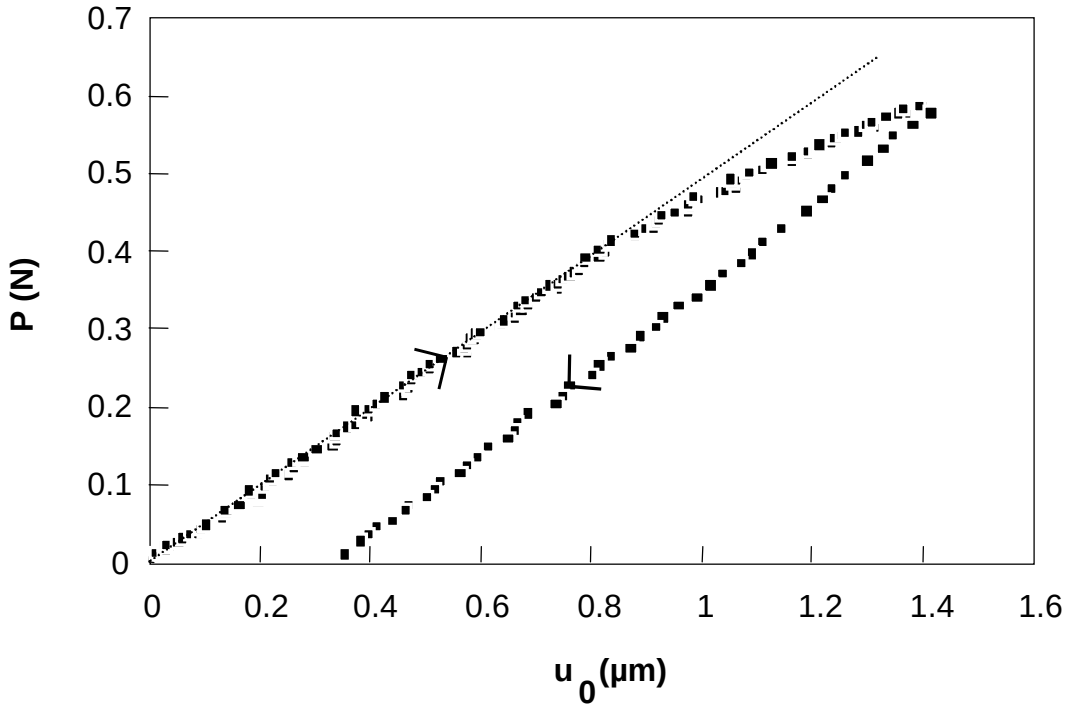

Fig. 4 : *Typical reduced indentation curve (composite S1).*

The two parameters of the model (n and τ_d) were identified from the reduced indentation curves. n was calculated from the initial linear part of the reduced curves using equation (2). It provided a quantitative assessment of the local fibre packing, which needs to be taken into account in any quantitative analysis of micro-indentation data [**10**]. The debonding strength τ_i was obtained by a least square fitting of the entire loading curve using expressions (2) and (4). For each material, about 20 indentation curves were treated individually using this procedure. Average values of τ_i are reported in Table 3. Contrary to macro-mechanical testing, it was found that micro-indentation was unable to reveal any significant difference between the three different sizing. Composites S1 and S2 exhibited interfacial shear strengths very close to the macro-mechanical values derived from ILSS tests. On the other hand, the interfacial shear strength of the material S3 was much greater than the ILSS and it can therefore not account for its low shear properties under impact and fatigue loading. The latter can rather be attributed to the existence of micro-structural defects in the materials.

Table 3: *Interfacial shear strengths measured using micro-indentation tests. (standard deviations within brackets).*

Sizing	Interfacial shear strength: τ_i (MPa)
S1	71 (5)
S2	70 (6)
S3	78 (3)

Discussion

Macro-mechanical tests revealed a strong difference in the damage development between composites S1 and S2 to one hand and composite S3 to the other hand. This difference was mainly related to the low shear properties of the composite processed with the sizing S3. This led to premature inter-laminar shear failure over a wide range of loading conditions including quasi-static, fatigue and impact loading. On the other hand micro-mechanical tests did not provide any evidence of different fibre/matrix interfacial shear strengths between the three sizing.

These contradictory results can be explained if the material microstructure is considered. Fig. 5 shows S.E.M. observations of cross-sections of the composites S1 and S3. For composite S1, a relatively homogeneous distribution of the fibres within the matrix was achieved. On the other hand, a highly heterogeneous distribution was obtained in the case of the S3 sizing. Fibre bundles in matrix rich regions can easily be distinguished, together with numerous voids. This fibre distribution can be related to the poor wettability of the fibre by the epoxy matrix during the impregnation process.

This means that the main effect of the sizing was to affect the composite microstructure at the mesoscopic scale, rather than to change the intrinsic strength properties of the fibre/matrix interface. The most significant effect of the sizing was thus encountered during the impregnation stage of material manufacturing. Moreover, the fatigue and impact results demonstrate the high sensitivity of damage development to the distribution of the reinforcement within the matrix.

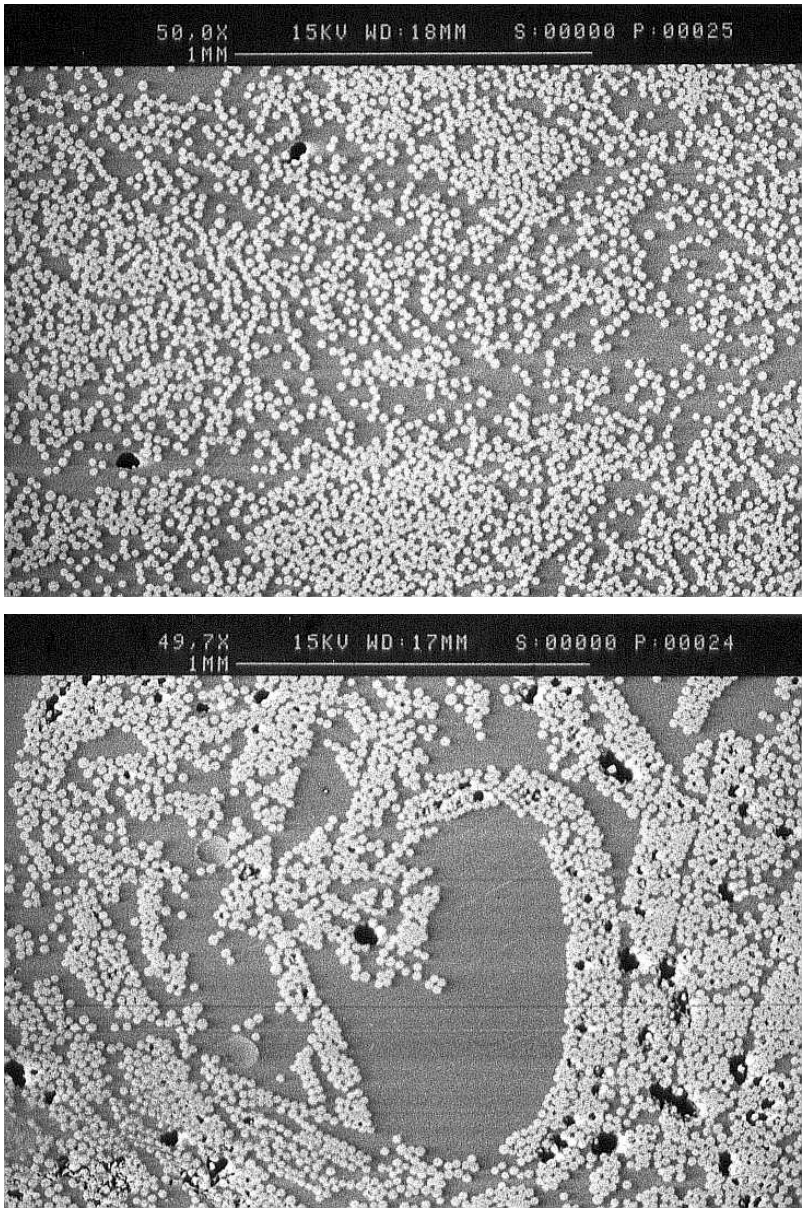

(a)

(b)

Fig. 5 : *S.E.M. observations of composites S1 (a) and S3 (b).*

CONCLUSION

Macro and micro-mechanical tests have been carried out using unidirectional glass/epoxy composites differing by their fibre surface treatments. Strong differences have been observed regarding damage development under fatigue and impact loading, whereas micro-indentation tests were unable to reveal any significant change in the interfacial shear strengths. These differences between the micro and macro-mechanical behaviour were interpreted by means of observations of the fibre distribution within the composite. By modifying the wettability of the fibre by the matrix during the impregnation process, the changes in the sizing resulted in very different microstructures. When a highly heterogeneous fibre distribution was achieved, the resulting low shear properties resulted in a drop in the fatigue and impact resistance. It must therefore emphasised that any assessment of the effects of fibre treatments on the interfacial properties from macro-mechanical tests can be misleading if it does not integrate a detailed analysis of the composite microstructure.

ACKNOWLEDGEMENTS

The authors fully acknowledge Vetrotex International (Chambery, France) for supplying the materials.

REFERENCES

1. Reifsnider, K.L., “Modelling of the interphase in polymer-matrix composite material systems”, *Composites*, Vol. 25, N° 7, 1994, pp.461-469.

2. Verpoest, I., Desaeger, M., Ivens, J., Wevers, M, “Interfaces in polymer matrix composites: from micromechanical tests to macromechanical properties”, *Makromol. Chem., Macromol. Symp.*, Vol. 75, 1993, pp. 85-98.

3. Pigott, M.R., “Why interface testing by single-fibre methods can be misleading”, *Composites Science and Technology*, Vol. 57, 1997, pp. 965-974.

4. Lacrampe, V., PhD Dissertation, Institut National des Sciences Appliquées de Lyon (INSA), France, 1992.

5. Kharrat, M., Chateauminois, A., Carpentier, L., Kapsa, Ph., “On the interfacial behaviour of a glass/epoxy composite during a micro-indentation test: assessment of interfacial shear strength using reduced indentation curves”, *Composites Part A*, Vol. 28A, 1997, pp. 39-46.

6. Berg, C.A., Tirosh, J., Israeli, M., “Analysis of short beam bending of fiber reinforced composites”, *ASTM STP 497*, American Society for Testing and Materials, Philadelphia, 1972, p. 206-218.

7. Chateauminois, A., Chabert, B., Soulier, J.P., Vincent, L., "Hygrothermal ageing effects on the static fatigue of glass/epoxy composites", *Composites*, Vol. 24, N° 7,1993, pp.547-555;

8. Desaeger, M., Verpoest, I., “On the use of the micro-indentation test technique to measure the interfacial shear strength of fibre-reinforced polymer composites”, *Composites Science and Technology*, Vol. 48, 1993, pp. 215-226.

9. Zidi, M., Carpentier, L., Chateauminois, A., Sidoroff, F., “Quantitative analysis of the micro-indentation behaviour of fibre reinforced composites: Development and validation of an analytical model”, Submitted to *Composite Science and Technology*.

10. Mandell, J.F., Grande, D.H., Tsiang, T.H., McGarry, F.J, “Modified micro-debonding test for direct in situ/fiber matrix bond strength determination in fiber composites”, *Composite Materials: Testing and Design (Seventh Conference), ASTM STP 893*, J. M. Whitney, J.M., Ed., American Society for Testing and Materials, Philadelphia, 1986, pp. 87-108.